Applied Catalysis B: Environmental 165 (2015) 192–199

Contents lists available at ScienceDirect

Applied Catalysis B: Environmental

journal homepage: www.elsevier.com/locate/apcatb

Deactivation of Cu/SAPO-34 during low-temperature NH_3-SCR

Kirsten Leistner, Louise Olsson *

Chemical Reaction Engineering, Competence Centre for Catalysis, Chalmers University of Technology, SE-412 96 Gothenburg, Sweden

ARTICLE INFO

Article history:
Received 20 May 2014
Received in revised form
23 September 2014
Accepted 25 September 2014
Available online 6 October 2014

Keywords:
Cu/SAPO-34
Deactivation
Hydrothermal stability
Ammonia SCR
Water

ABSTRACT

The sensitivity of NH_3-SCR activity to water vapour at 70 °C is tested for Cu/SAPO-34 (morph.) catalysts. The synthesised Cu/SAPO-34 (morph.) is remarkably susceptible to low-temperature activity loss. After only 3 h at 70 °C, the NO_x conversion decreases from an initial 87% to 66% at 200 °C, after another 9 h to 6%. This deactivation is accompanied by a partial loss of microporous volume, but the SAPO-34 framework remains crystalline. We postulate that a transformation of the active copper sites into an inactive form could be the cause for the deactivation. Regeneration of the catalyst was attempted, but had no impact on activity.

1. Introduction

In the current framework of increasingly stringent emission regulations, the development of efficient catalysts for selective catalytic reduction (SCR) in lean-burn engine exhausts is critical. One of the major issues to be overcome when developing new catalysts is catalyst deactivation, which usually results in loss of activity and selectivity [1]. Deactivation can result from competitive adsorption of certain molecules on SCR sites, thereby inhibiting the SCR reaction, or from thermal degradation such as sintering (in the case of noble metals) and dealumination (in the case of zeolites) occurring at high temperatures (>600 °C) [1,2]. It is commonly thought that adsorbed ammonia or water preventing adsorption of nitric oxide is responsible for low-temperature inhibition observed over copper-exchanged zeolites [3–5]. However, this type of deactivation can be reversed by raising the temperature. On the other hand, activity loss due to thermal degradation may be permanent, making hydrothermal stability one of the most important characteristics of an NH_3-SCR catalyst. High temperatures recur in fact quite frequently in commercial applications, since diesel particle filters (DPFs) are often placed upstream of the SCR catalyst [6]. The evolution of SCR catalysts over time has been in large part due to the need for greater stability at high temperatures: the initially popular metal oxides have been partially replaced by copper and iron-exchanged zeolites which are stable at higher temperatures (up to 600 °C) [7,8]. Most recently, attention has shifted from the established large and medium pore zeolites to include zeolites and other molecular sieves with small-pore frameworks [9]. Of these, the two most prominent are Cu/SSZ-13 and Cu/SAPO-34, which are stable after steaming at 800 °C [10–12]. Their superior hydrothermal stability has repeatedly been attributed to the small size of their pores, which prevents detached $Al(OH)_3$ moieties from exiting the framework. Once the catalyst is cooled down again, the aluminium hydroxide moiety settles back into the framework, and dealumination has thus been averted because the framework stays intact [9,13,14].

While stability is largely a high temperature issue for most zeolites, there have been some early reports of poor stability in silicoaluminophosphates (SAPO-*n*) exposed to a relative humidity above 40% at room temperature [15,16]. These studies found an often reversible loss of crystallinity and porosity upon low-temperature hydration of pure SAPO-34 powders and membranes. SAPO-34 is also known to be prone to hydrolysis when undergoing aqueous ion exchange [17]. This is particularly pronounced for catalysts synthesised using morpholine as a template (rather than triethylamine), because of the higher framework charge density and stress [17]. However, the low temperature hydrostability of copper-exchanged SAPO-34 in conditions relevant to NH_3-SCR (smaller relative humidity, temperature between room temperature and 100 °C) has, to our knowledge, not been studied. Stability at temperatures below 100 °C is important for SCR applications, especially during startup, when the working temperature has not

* Corresponding author. Tel.: +46 31 772 4390; fax: +46 31 772 3035.
E-mail addresses: leistner@chalmers.se (K. Leistner), louise.olsson@chalmers.se (L. Olsson).

http://dx.doi.org/10.1016/j.apcatb.2014.09.067
0926-3373/

yet been reached. The objective of this study has therefore been to examine the effect of a low-temperature SCR atmosphere (including water vapour) on the short and longer-term performance of a Cu/SAPO-34 catalyst.

2. Experimental procedure

2.1. Catalyst preparation

Two batches of SAPO-34 were prepared and then exchanged to produce two batches of Cu/SAPO-34 with different copper loadings (1.27 and 2.60 wt.%). SAPO-34 was first prepared by hydrothermal synthesis from a gel with the following molar composition: Al_2O_3:1.06 P_2O_5:1.08 SiO_2:2.09 morpholine:66 deionised H_2O. Pseudoboehmite (Pural SB-1, Sasol), H_3PO_4 (Merck) and colloidal silica (Ludox AS-40, Aldrich) were used as the aluminium, silicon and phosphorus sources, respectively and morpholine (Sigma–Aldrich) was the structure directing agent (SDA). Initially, H_3PO_4 (27.8 g, 85%) was dissolved by stirring in 115.7 g water for 15 min and then the pseudoboehmite (15.7 g) was added slowly over 2 h, under continuous agitation. Stirring was then continued for another 12 h, until a uniform gel was obtained. In the next step, a second solution of colloidal silica (18.4 g) and morpholine (21.1 g) was prepared, which was then slowly added to the first solution over 1 h and under constant stirring. The resulting slurry was stirred for another 7 h and then aged for 24 h at room temperature without stirring. For the crystallization process, the mixture was transferred to a Teflon-lined stainless steel autoclave and heated for 72 h at 200 °C, under autogenic pressure. After crystallization, the product was left to cool to room temperature, and the solid part was then washed thoroughly with deionised water and filtered by centrifugation. The end product was ground to a fine powder and calcined in air at 560 °C for 6 h.

The resulting SAPO-34 powder was twice subjected to ion exchange with a 5.4 M solution of NH_4NO_3 (Sigma–Aldrich). These ion-exchanges were performed at 80 °C using 70 ml of ammonium nitrate solution per 10 g of SAPO-34 and the pH was buffered during the process to stay between 3.0 and 3.5. A third ion-exchange with a solution of $Cu(NO_3)_2$ (Alfa Aesar) was carried out at 70 °C (4 ml of copper nitrate solution per gram of NH_4/SAPO-34). The concentrations of the solutions were 0.2 and 0.8 M for the two batches attaining 1.27 and 2.60 wt.% Cu, respectively and the solution was buffered only to prevent the pH from deviating from the desired range of 3.0–3.5. After each of these exchanges, the powder was thoroughly washed with deionised water, filtered by centrifugation and then dried at 90–100 °C for at least 12 h. Finally, the powder was calcined in air: at 550 °C for 3 h and, in the case of the powder with Cu wt.% of 2.6%, a second calcination was performed at 750 °C for 2 h. The catalysts are denoted as Cu/SAPO34 (morph.) to indicate that morpholine was used as a template.

For the activity experiments, the Cu/SAPO-34 (morph.) powders were coated on monoliths cut from commercial honeycomb cordierite (length: 20 mm, diameter: 21 mm, cell density: 400 cpsi). The coating of the catalysts was preceded by coating of an alumina layer (Disperal D, Sasol). In both instances, the impregnation was performed by repeated dipping in a slurry consisting of 95% liquid phase (equal parts deionised water and ethanol) and 5% solid phase (Cu/SAPO-34 and/or Disperal D). After each dipping, excess slurry was blown away and the monolith dried for 3 min at 90 °C. When the desired washcoat mass had been obtained, the monoliths with Cu/SAPO-34 (morph.)—1.27 and 2.60 wt.% were calcined in air for 2 h at 500 and 750 °C, respectively. Further details on catalyst and monolith preparation are available in a previous publication [18].

2.2. Activity measurements

All the activity experiments are reactor experiments, where the monolith was wrapped in quartz wool to prevent slip and then inserted in a horizontal quartz reactor tube approximately 800 mm long and with an internal diameter of 22 mm. The reactive gas mixture at the inlet to the reactor (Ar as balance, NH_3, NO and/or water vapour) was regulated using Bronkhorst massflow controllers (MFCs) and water vapour was produced by a controlled evaporation and mixing system (CEM, Bronkorst). The mole fractions of the product gases NH_3, NO, NO_2, N_2O and H_2O were measured at the outlet of the reactor by a MKS^{TM} multigas 2030 FTIR spectrometer. The reactor temperature was controlled by a heating unit consisting of a Eurotherm controller, a heating coil placed around the reactor tube and a power supply. Additionally, the reactor tube was wrapped in quartz wool in order to maintain the set temperature. Catalyst and gas temperature during the activity experiments were measured by two K-type thermocouples located inside a central channel of the monolith and 10 mm upstream of the monolith, respectively. All lines upstream and downstream of the reactor were heated to 150 or 200 °C to prevent condensation of water vapour. The system was operated at a total flow rate of 3500 ml/min, corresponding to a gas hourly space velocity (GHSV) of 30330 h^{-1}, based on the monolith volume. Prior to the first experiment, each monolith was degreened in a 4 h-long exposure to 400 ppm NH_3, 400 ppm NO, 8% O_2 and 5% H_2O at 700 °C to ensure stable activity. Before each experiment, the catalyst surface was cleaned by a high-temperature pre-treatment. The experiments were of two types: step-wise activity tests and adsorption/desorption tests. During the activity tests, the reaction temperature was varied in steps and each step was held long enough to allow for observation of steady state concentrations. Table 1 summarises all reactor experiments carried out in this study together with their pre-treatment conditions in the order of execution. The temperatures used are comprised between 70 and 200 °C. At 70 °C, the water content used for the feed gas, 5%, corresponds to a relative humidity of 16.2%.

2.3. Catalyst characterisation

The synthesised catalysts were characterized using Brunauer–Emmett–Teller measurements (BET), microporous volume measurements, X-ray diffraction (XRD), UV–visible spectroscopy (UV–vis), temperature-programmed reduction (TPR) and Inductively Coupled Plasma Sector Field Mass Spectrometry (ICP-SFMS). ICP-SFMS was used to determine the elemental composition of the catalysts before the experiments, and was carried out by ALS Scandinavia AB. Nitrogen adsorption–desorption at 77 K for BET and pore volume measurements were performed using a Tristar 3000 (Micromeritics) instrument. Prior to the measurement, the samples were outgassed under vacuum at 220 °C for 3 h. The X-ray diffractograms were obtained using a Bruker AXS D8 advance operating at 40 kV and 40 mA with nickel-filtered Cu Kα radiation (λ = 1.5418 A) in the range $5° < 2\theta < 40°$ with a step size of 0.029°. The Hall–Williamson method (accounting for broadening due to strain, but not instrumental broadening) was employed to calculate crystallite size from the diffraction peaks using a value of $k = 1$. The peaks at 2θ = 9.7, 13, 16.2, 18, 20.8, 25.3 and 26.1° were used in the analysis, and the FWHM and centre of said peaks determined by fitting the experimental peaks with a Gaussian distribution. UV–vis spectra were acquired using a Cary 5000 UV–vis NIR spectrophotometer in the diffuse reflectance (DR) mode. The TPR experiments were carried out in a Setaram Sensys DSC (Digital Scanning Calorimeter). Two quartz tubes were mounted inside the DSC. In one tube, ca. 60 mg of catalyst powder was placed on a porous quartz frit. Bronkhorst MFCs were used to

Table 1
Experiments performed in this study, in the order of execution.

Catalyst	Pre-treatment	Exp. n.	Feed	Temperature protocol (°C)
1.27 Cu wt.%	20 min under 8% O_2, 5% H_2O at 600 °C	1	400 ppm NH_3, 400 ppm NO, 8% O_2, 5% H_2O	150, 200, 150, 125, 100, 70, 100, 125, 150, 200
		2	400 ppm NH_3, 400 ppm NO, 8% O_2, 5% H_2O	150, 200, 150, 125, 100, 70, 100, 125, 150, 200
2.60 Cu wt.%	20 min under 8% O_2 at 600 °C 15 min under 100% Ar at 600 °C	3	Adsorption under 400 ppm NH_3 TPD under 100% Ar	Adsorption at 70 °C TPD at 10 °C/min
		4	400 ppm NH_3, 400 ppm NO, 8% O_2, 5% H_2O	150, 200, 150, 70, 150, 200
		5	400 ppm NH_3, 400 ppm NO, 8% O_2	150, 200, 150, 70, 150, 200
		6	400 ppm NH_3, 400 ppm NO, 8% O_2 at 150 and 200 °C 5% H_2O at 70 °C	150, 200, 150, 70, 150, 200
		7	Adsorption under 400 ppm NH_3 TPD under 100% Ar	Adsorption at 70 °C TPD at 10 °C/min
		8	Adsorption under 400 ppm NH_3, 5% H_2O TPD under 100% Ar, 5% H_2O	Adsorption at 70 °C TPD at 10 °C/min
		9	400 ppm NH_3, 400 ppm NO, 8% O_2 at 150 and 200 °C 5% H_2O at 70 °C	150, 200, 150, 70 (2 h), 150, 200
		10	400 ppm NH_3, 400 ppm NO, 8% O_2 at 150 and 200 °C 5% H_2O at 70 °C	150, 200, 150, 70 (4 h), 150, 200
		11	400 ppm NH_3, 400 ppm NO, 8% O_2 at 150 and 200 °C	150, 200

mix the reactive gases and the carrier gas argon ahead of the DSC and a flow of 20 ml/min was sent into each of the two tubes. A Hiden HPR-20 QUI mass spectrometer (MS) was used to measure the H_2 mole fraction at the exit of the catalyst-containing tube. Prior to each measurement, the surface of the catalyst was cleaned by exposing it to 8% O_2 at 600 °C for 1 h. The tube was then cooled down to 50 °C under Ar. Then 0.3% of H_2 were introduced into the flow and the temperature kept at 50 °C for 30 min. Thereafter the temperature was raised to 800 °C at a ramping rate of 10 °C/min and then kept at 800 °C for a further 20 min, still under 0.3% of H_2. XRD, UV–vis, TPR and BET measurements were performed both on the fresh powder sample preceding the reactor experiments and on the deactivated catalysts scraped off the monoliths. In the case of the TPR, the fresh catalyst powders were degreened for 4 h under 400 ppm NO and 8% O_2 prior to surface cleaning.

3. Results and discussion

In experiment n. 1, Cu/SAPO-34 (morph.) with Cu wt.% 1.27 was exposed to typical wet standard SCR conditions, preceded by a 600 °C-pre-treatment intended to clean the catalyst's surface from any adsorbed species (see Table 1). During the experiment itself, the temperature was first kept at 150 °C, then 200 and 150 °C again, before being brought down to 70 °C via a number of intermediate steps, and then back up to 150 and 200 °C. Ammonia and nitric oxide consumption and the measured temperature profile for this experiment are shown in Fig. 1a. The NH_3 and NO mole fractions reach the same steady state values both at the first and second 150 °C-step, and NO_x conversion as shown in Table 2 is 10% at 150 °C and 21% at 200 °C. The temperature is then decreased further to 125, 100 and a minimum of 70 °C and conversion goes to zero at 100 and 70 °C. After the step at 70 °C, the temperature is once more raised, ending with 150 and 200 °C, but it is apparent from the NH_3 and NO profiles in Fig. 1a that conversion is now significantly lower than it was

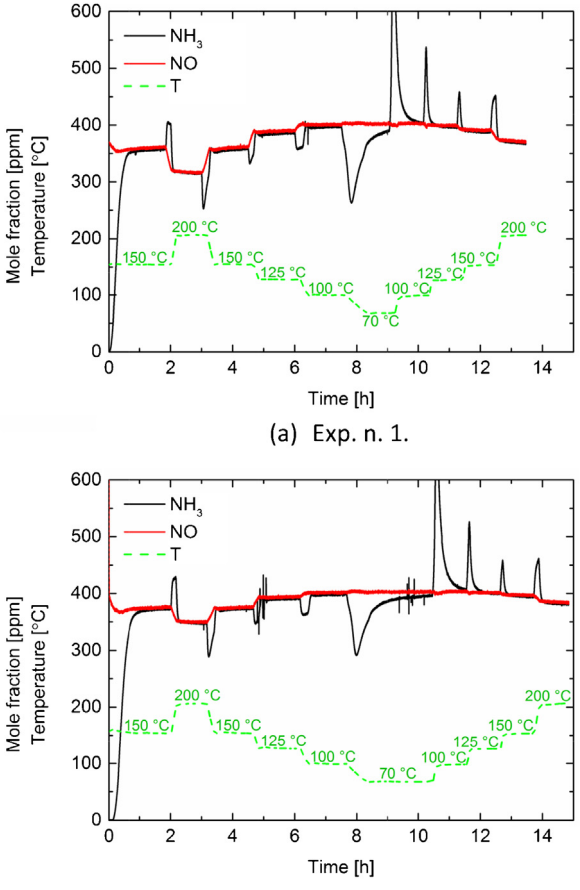

Fig. 1. Stepwise NH_3-SCR over Cu/-SAPO-34 (morph.)—1.27 Cu wt.%. Feed: 400 ppm NH_3, 400 ppm NO, 8% O_2, 5% H_2O.

Table 2
Changes in NO_x conversion upon exposure to water vapour at 70 °C.

Catalyst	Exp.	Before exposure to water vapour at 70 °C		After exposure to water vapour at 70 °C	
		150 °C	200 °C	150 °C	200 °C
1.27 Cu wt.%	1	10%	21%	3%	8%
	2	6%	13%	1%	4%
2.60 Cu wt.%	4	47%	87%	22%	66%
	5	55%	80%	44%	70%
	6	37%	71%	14%	47%
	9	7%	15%	1%	6%
	10	2%	5%	2%	4%
	11	1%	4%		

before at the same temperatures (3 and 8%, instead of 10 and 21% as before). This indicates that some sort of deactivation is occurring.

The experiment was subsequently repeated on the same catalyst (the only difference is that the step at 70 °C was held for 2.2 h instead of 1 h) and the results are shown in Fig. 1b. Before the repeat, the catalyst surface was cleaned by the same high-temperature pre-treatment of 20 min under 8% O_2 and 5% H_2O. The observed behaviour is qualitatively analogous to the first experiment, with NO and NH_3 consumption being greater before reaction at 70 °C (conversion 6 and 13%) than after (1 and 4%). However, the NO_x conversion during the first two temperature steps is already lower than it was during the first two steps of experiment n. 1 (Fig. 1a): At 200 °C, the conversion is only 13%, compared with 21% during the first repetition. The observed deactivation is therefore greater at the second repetition, which could indicate that the pre-treatment did not remove all adsorbed species or that the deactivation is of a more permanent nature.

To test the repeatability of the observation, similar experiments were carried out on a batch of Cu/SAPO-34 (morph.) with the higher copper loading of 2.60 wt.%. There was a small possibility that the pre-treatment with water might result in water left on the surface, contributing to the deactivation. In order to ensure that this was not the case a different pre-treatment was employed for Cu/SAPO-34 (morph.)—2.60 wt.%, where the catalyst was pre-treated for 20 min at 600 °C with 8% O_2 in absence of H_2O. A second step of cleaning with argon only was also added, see Table 1. The first experiment (exp. n. 3) performed on the second catalyst was an adsorption test with 400 ppm NH_3. The second (exp. n. 4) was a stepwise experiment in wet standard SCR conditions; the results of this SCR experiment are shown in Fig. 2a. The only difference to the previous experiments is that it contained fewer temperature steps. Again, the results are comparable with those of exp. n. 1 and 2: Conversion at 150 °C goes from 47% before exposure at 70 °C to 22% after exposure. At 200 °C, the value of the conversion drops from 87% to 66%. The deactivation observed upon reaction at 70 °C in a wet atmosphere for both Cu/SAPO-34 (morph.) catalysts appears to be in line with an early report of low-temperature sensitivity of SAPO-34 powders, although these were steamed in much more highly humid atmospheres with no other feed gases [15]. It is also worth recalling the susceptibility of SAPO-34 to hydrolysis in aqueous solutions [17] and a report of decreased CO_2/CH_4 separation efficiency in SAPO-34 membranes exposed to water vapour [16]. Given these studies, it seems likely that the loss of activity observed here is caused by the presence of water. To test this hypothesis, exp. n. 5, a stepwise SCR experiment in dry atmosphere, was performed next. Its results are shown in Fig. 2b. Compared to the results from a wet atmosphere, the results for the dry atmosphere before hydration at 70 °C exhibit higher conversion at 150 °C (55% versus 47%), but lower conversion at 200 °C (80% versus 87%). (It is thinkable that this effect may be due to competitive adsorption of water and NH_3/NO, as has been observed on other zeolites [2,19,20]. It is not possible to comment with any certainty on the effect of water on

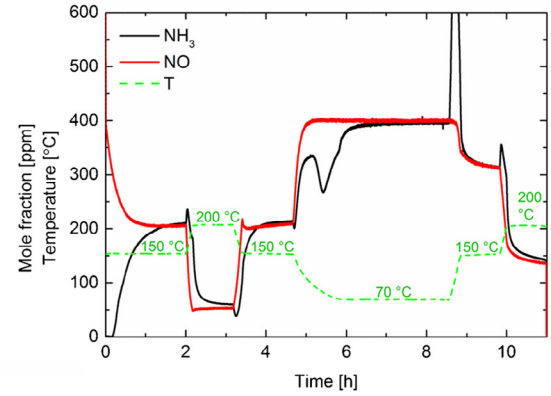

(a) Exp. n. 4. Feed: 400 ppm NH_3, 400 ppm NO, 8% O_2, 5% H_2O.

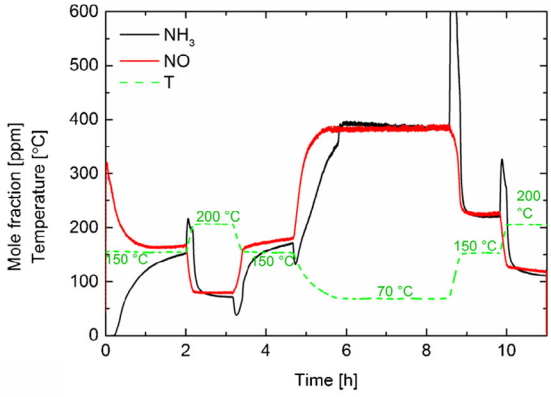

(b) Exp. n. 5. Feed: 400 ppm NH_3, 400 ppm NO, 8% O_2.

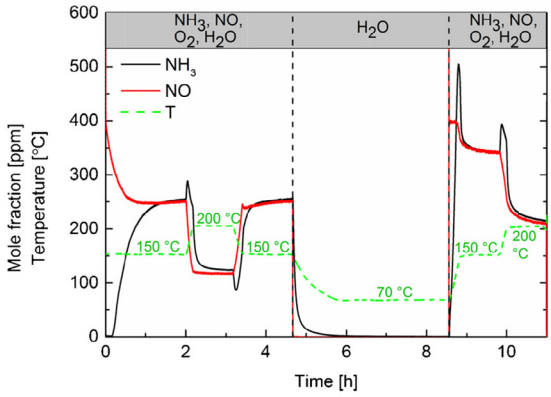

(c) Exp. n. 6. Feed: At 70 °C: only 5% H_2O, at other temperatures 400 ppm NH_3, 400 ppm NO, 8% O_2, 5% H_2O.

Fig. 2. Stepwise NH_3-SCR over Cu/-SAPO-34 (morph.)—2.60 Cu wt.%.

the SCR mechanism here, because of the decline in activity of the catalyst throughout experiments n. 4–6.) Fig. 2b also shows that contact with a dry atmosphere at 70 °C does cause some loss of activity at 150 and 200 °C, but less so than the wet atmosphere. For instance, at 200 °C, conversion is reduced from 80 to 70%. While it is possible that this smaller deactivation is attributable to ammonia inhibition or ammonia interacting with SAPO-34 [21], it is presumably more likely that it is caused by water produced by the SCR reaction $4NH_3 + 4NO + O_2 \rightarrow 4N_2 + 6H_2O$.

The hypothesis of water causing the deactivation was tested by performing another wet SCR experiment (exp. n. 6), where however NH_3 and NO were cut off from the feed throughout the step at 70 °C, so that water vapour was the only reactive feed component, as shown in Fig. 2c. The steps prior to 70 °C indicate a clear deterioration of activity at 150 and 200 °C, with respect to exp. n. 4 (Fig. 2a). At 200 °C, the conversion has dropped from 87% to 71%. This is the same difference in behaviour observed for the first catalyst (exp. 1 and 2). The second catalyst has been pre-treated at 600 °C in an atmosphere free of water. Despite this, the initial level of activity is not fully regained. This suggests that the observed deactivation may be, at least partially, permanent. Permanent loss of activity was found in some cases on SAPO-34, where XRD diffractograms showed that the crystalline structure had been destroyed by the action of water [22]. The suggestion that water is responsible for the deterioration of SCR activity is supported by the observation in Fig. 2c and Table 2 that the drop in conversion upon exposure at 70 °C is again much greater than for a dry atmosphere (71% before and 47% after).

Three ammonia temperature programmed desorption (TPD) tests at 70 °C were performed on Cu/SAPO-34 (morph.) (2.60 wt.%). The first to be performed was exp n. 3, with NH_3 in absence of H_2O. It was followed by the three SCR experiments described earlier. After these experiments, the dry ammonia TPD test was repeated (exp. n. 7), with the intention of observing the effect of prolonged exposure at 70 °C on the adsorption capacity of Cu/SAPO-34 (morph.). Thereafter, ammonia adsorption was tested in the presence of water (exp. n. 8). Results from all three tests are shown in Fig. 3. The NH_3 profile from dry adsorption before any contact with water vapour at 70 °C (exp. n. 3) and after repeated contact (exp. n. 7) are practically identical. It therefore appears that at this stage, although SCR activity at 150 and 200 °C is to some extent permanently affected by water at low temperature, the adsorption capacity at 70 °C is not. When ammonia adsorption was repeated in presence of 5% H_2O (exp. n. 8), the adsorption capacity was slightly reduced, as seen in Fig. 3, from 4.2 to 3.4 mmol/g_{cat},. The difference is most noticeable for the weakly bound ammonia, desorbing when inlet ammonia is turned

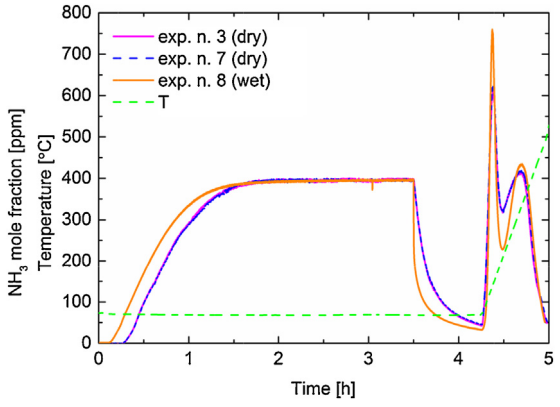

Fig. 3. NH_3-adsorption at 70 °C and TPD over Cu/-SAPO-34 (morph.)—2.60 Cu wt.%. Adsorption feed: Exp. 3 and 7: 400 ppm NH_3 and exp. 8: 400 ppm NH_3 and 5% H_2O. TPD heating rate: 10 °C/min.

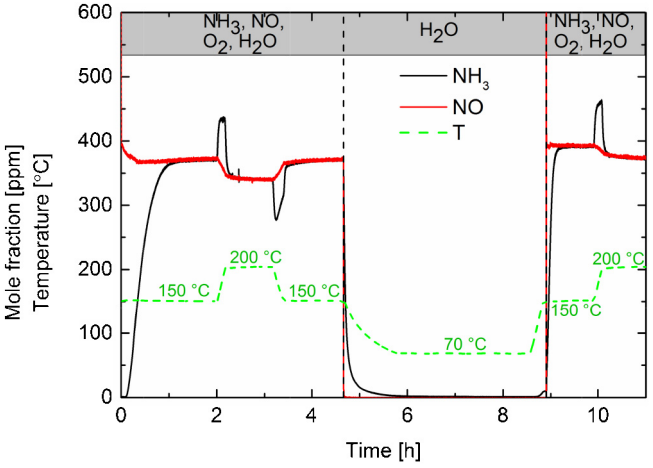

Fig. 4. Stepwise NH_3-SCR over Cu/-SAPO-34 (morph.)—2.60 Cu wt.% (exp. n. 9). Feed: At 70 °C: only 5% H_2O, at other temperatures 400 ppm NH_3, 400 ppm NO, 8% O_2, 5% H_2O.

off at 150 °C. It decreases from 1.2 to 0.72 mmol/g_{cat} due to water adsorption. But a small decrease in the ammonia desorption during the temperature ramp is also visible, with the storage decreasing from 3.0 to 2.8 mmol/g_{cat}. The decreased ammonia storage in the presence of water is likely due to competitive adsorption on the same sites. However, in both exp. n. 7 and 8, the ammonia adsorption capacity is still significant, and in view of this and the previous observation that the deactivation is linked to the presence of water, it appears likely that the loss of activity is not caused by NH_3 or NO blocking adsorption sites.

Finally, in exp. n. 9, the procedure of exp. n. 6 where only water was present in the feed during the 70 °C temperature step, was repeated. The results in Fig. 4 show that activity is now greatly diminished. Indeed, the highest conversion is reached at 200 °C before the 70 °C step, and it is only 15%. This is probably owing to the prolonged exposure during the adsorption phase of exp. n. 8 (3.5 h). The same experiment was again repeated, but with a longer time (4 h) at 70 °C, with the intent of severely deactivating the catalyst. The results of this test (exp. n. 10) during the 200 °C step, before the deactivation step, gave a conversion of only 5% (results not shown), and when the surface was cleaned and the first steps of the experiment repeated again (exp. n. 11), the conversion dropped to 4%, compared to the initial conversion of 87%. Thus an extremely large deactivation has occurred.

After the deactivation experiments, both catalysts were scraped off the monoliths in order to perform XRD and BET analyses. As pointed out earlier, it seems improbable that NH_3 or NO are blocking adsorption sites on Cu/SAPO-34 (morph.), given the pretreatment at 600 °C. Hence one possibility was that the loss of activity brought on by contact with water at low temperatures is caused by destruction of the crystalline SAPO-34 framework. This was found to be the case for H/SAPO-34 hydrated at 110 °C, and SAPO-34 hydrated at temperatures between room temperature and 100 °C [15,22]. Here, however, the X-ray diffractograms in Fig. 5 show that the crystalline structure of both catalysts is similar, as all the characteristic peaks of the SAPO-34 structure remain visible after deactivation. The principal difference between the patterns before and after deactivation is in the peak height, but this could be due to different particle shape or packing after scraping the coated catalyst off the monoliths, as compared to the fresh, uncoated powder. However, BET area and porosity are reduced after the deactivation, see Table 3. It should be noted that the scraped off wash-coat used for the deactivated samples contains small amounts of binder (5%) and could also contain minor

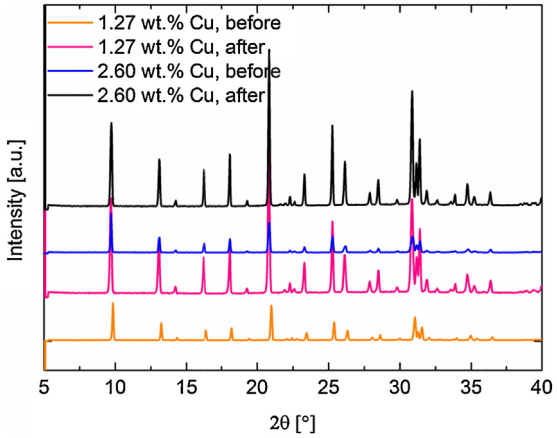

Fig. 5. XR diffractograms before and after exposure to water vapour at 70 °C.

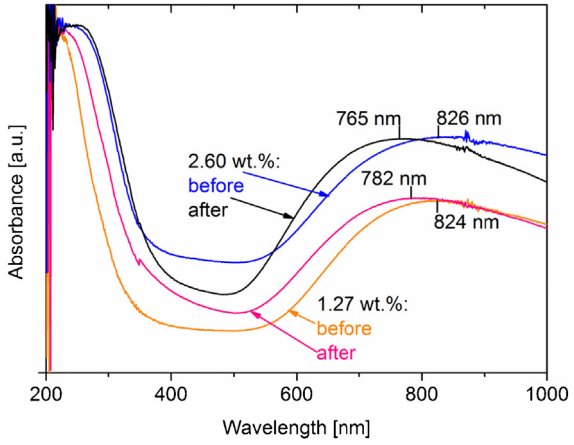

Fig. 6. UV–vis spectra before and after exposure to water vapour at 70 °C.

amounts of the thin alumina layer described in Section 2.1. If all alumina in the inner layer were scraped off, which is unlikely, the sample would contain a maximum of 13% alumina and thus the remaining part, 87%, is the zeolite. For a Pt/Al_2O_3 powder catalyst, we have previously obtained a surface area of 158 m^2/g and a pore volume of 0.0054 cm^3/g. Using these data and the maximum available alumina (13%) to estimate the surface area and pore volume for the combined zeolite and alumina we obtain a BET area of 527 and 494 m^2/g and a pore volume of 0.24 and 0.22 g/cm^3, respectively. The measured values for the deactivated samples are significantly lower for 1.27 wt.% Cu-SAPO-34 where the BET decreased by at least 20% and pore volume by at least 24% when compensating for alumina content. However, for the 2.60 wt.% Cu-SAPO-34 sample the corresponding decrease is 4 and 8%, respectively. To conclude, it is possible that the structure is somewhat affected by the deactivation, since the BET surface area and pore volume decreased, even though changes are not clearly visible in the XRD pattern. However, for 2.60 wt.% Cu-SAPO-34 the changes after deactivation are small.

Briend et al. found that SAPO-34 exposed to high relative humidities at room temperature lost its microporosity gradually with hydration time [15]. Time of total loss of porosity varied between 10 and 1000 days, depending on sample composition/method of synthesis. In our study, Cu/SAPO-34 (morph.) – 1.27 wt.% was exposed to humidity at 70 °C for a total of 15 h, and Cu/SAPO-34 (morph.) – 2.60 wt.% for 14 h. This is in line with Briend's findings [15]. Note that these times take into account some additional experiments performed on Cu/SAPO-34 (morph.) – 1.27 wt.%, which are not shown here. Briend et al. found that severe loss of crystallinity and porosity could occur reversibly or irreversibly, depending on time of hydration and sample composition [15]. After 1–2 days of exposure to moisture, crystallinity and porous volume were not recoverable any longer upon high temperature treatment [15]. Briend et al. attributed the deterioration of the framework to the breakage of Si–OH–Al bonds at low temperature [15]. A comparison of exp. n. 4 and 6 in this study shows that the loss of activity here is only to a small extent reversible with the pre-treatment at 600 °C. Thus, a conversion of 66% is obtained at the end of exp. n. 4, and 71% at the beginning of the later exp. n. 6.

It is interesting to note that the ammonia adsorption and TPD experiment on Cu/SAPO-34 (morph.)—2.60 wt.% (experiment n. 7, compared to n. 3) was not affected by the exposure to a low-temperature humid atmosphere, even though SCR activity on the same catalyst was severely compromised. One possible reason for this is that the nature of the copper sites, on which SCR occurs, is somehow modified, while the Brønsted acid sites, on which most of the ammonia is adsorbed, remain unchanged. In order to characterise the Cu species, UV–vis DR spectra of the two catalysts were acquired both before and after the deactivation occurred, and the results show in Fig. 6. Several studies have assigned a charge transfer band at around 225 nm to the $O_{SAPO-34} \rightarrow Cu^+/Cu^{2+}$ charge transition [23–25]. A broad band centered at around 800 nm has been assigned to the d→d transition of copper in the form of Cu^{2+}, and also coincides with the bands observed in the reference material $Cu(OH)_2$ [23–26]. Both the active and deactivated catalysts display these two major bands. On some Cu/SAPO-34 catalysts, two bands at 355 and 456 nm have been attributed to O–Cu–O and Cu–O–Cu complexes [25]. In Fig. 6, it appears as though deactivation may have increased the numbers of one or both of these oxidic complexes on Cu/SAPO-34 (morph.) – 1.27 wt.%. The opposite is observed for Cu/SAPO-34 (morph.) – 2.60 wt.%. However, copper oxide species on SAPO-34 are probably not connected with the deactivation, because it has been shown that they are readily transformed into the active Cu^{2+} upon high temperature treatment [25,27,28]. Perhaps the most significant change seen in the UV–vis spectra of both catalysts after deactivation, is a blueshift of the d→d transition band ascribed to Cu^{2+}. Nevertheless, the UV–vis data are not conclusive as to the copper deactivation mechanism.

To obtain more information on the copper species, H_2-TPR was therefore carried out on the fresh catalysts and the deactivated form scraped off the monoliths. The hydrogen consumption is shown in Fig. 7 and integration of these curves shows that the H_2/Cu ratio is approximately 0.5 for the two fresh catalysts (0.51 and 0.58 for Cu/SAPO-34 (morph.) – 2.60 wt.%. and Cu/SAPO-34 (morph.) – 1.27 wt.%, respectively). This indicates that all the Cu^{2+} ions have undergone a one-electron reduction. A significant difference is seen between the fresh and deactivated forms: the amount

Table 3
Changes in N_2-adsorption and crystallite properties upon exposure to water vapour at 70 °C.

Cu/SAPO-34 Cu loading (wt.%)	Hydration time at $T < 100$ °C (h)	BET surface area before hydration (m^2/g)	BET surface area after hydration (m^2/g)[a]	Micropore volume before hydration (cm^3/g)	Micropore volume after hydration (cm^3/g)[a]	Crystallite size before hydration (nm)	Crystallite size after hydration (nm)[a]
1.27 wt.%	15	582	420	0.27	0.18	102	75
2.60 wt.%	14	544	473	0.25	0.20	133	75

[a] Measurements done on scraped off wash-coat which contains up to 13% alumina from the binder (5%) and the thin alumina layer.

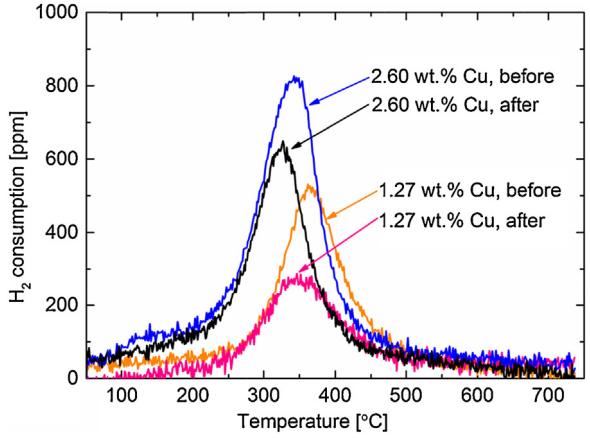

Fig. 7. H_2 consumption during H_2-TPR performed before and after exposure to water vapour at 70 °C. Feed: 0.3% H_2 in Ar. TPR performed from 50 to 800 °C with a heating rate of 10 °C/min.

of hydrogen consumed decreased by 26 and 38% after deactivation, for the higher and lower Cu loading, respectively. It should be noted that the scraped off wash-coat contains maximum of 13% alumina, due to binder and the thin inner alumina layer. Thus, since the decrease in hydrogen consumption in the TPR is significantly larger than 13%, i.e. 26 and 38%, the results clearly show that fewer copper ions are available for reduction after deactivation.

The activity experiments show that our synthesised Cu/SAPO-34 (morph.) is deactivated upon 14–15 h exposure to 70 °C, under SCR conditions with a moisture content representative of what may be found in engine exhaust [29]. Regeneration of the catalyst in dry conditions at high temperature (600 °C) was attempted, but not successful. Nevertheless, the main reason for the deactivation does not appear to be a loss of crystallinity of the SAPO-34 structure, based on XRD measurements. It is possible that breakdown of the crystal framework would appear after exposures longer than 15 h, as was observed by Briend et al. [15]. However, a remarkable loss of activity occurs before any significant loss of crystallinity can be observed by XRD (all characteristic SAPO-34 peaks are present). It should be noted that the BET surface area and pore volume decreased by at least 20 and 24%, respectively (after compensating for alumina content) for 1.27 wt.% Cu-SAPO-34 after deactivation. It is therefore possible that some structural changes are occurring, even though not clearly visible in the XRD. However, the decrease in BET and pore volume is significantly less for 2.60 wt.% Cu-SAPO-34 (4 and 8%) and consequently the structure is likely intact. Both these samples exhibit the same trends regarding deactivation and we can therefore conclude that structural changes are not the dominating mechanism for deactivation.

Pore plugging and inhibition are alternative explanations for the lowering of BET area and pore volume. However, inhibition of the SCR reaction by other species adsorbed on the catalytic sites seems unlikely, because such species would probably be removed during the regeneration attempts at 600 °C. Indeed, water inhibition should be removable by heat treatment of up to 500 °C, and even dealumination, if reversible, is reversible at 600 °C [2,15,30,31]. Similarly, the treatment at 600 °C would likely remove any obstructive species (such as ammonium nitrates, for e.g.) from the pores [18]. Further, if any pores are plugged, one would expect this to hinder access to Brønsted acid sites as well, not only to SCR active sites. Yet NH_3 storage and release was seen not to be impacted in any way.

The TPR experiments demonstrate that after deactivation less copper is available to undergo a reduction. The redox properties of copper are critical for the SCR activity and therefore a loss of this capability would be detrimental for the activity. On the other hand, it should be noted that the activity of both catalysts is reduced remarkably: from 87 to 4% in the case of Cu/SAPO-34–2.60 wt.% at 200 °C. It seems reasonable to suppose that the loss of 26 and 38% of the reducible copper species (note that a decrease of 13% might originate from alumina presence in the deactivated samples) is not alone responsible for this almost complete loss of activity. It is therefore possible that many of the copper sites are transformed into an inactive form.

4. Conclusions

In this study we have examined the low-temperature stability of Cu/SAPO-34 (morph.) with 1.27 and 2.60 wt.% Cu in ammonia-SCR conditions. We observed that after a few hours of exposure to a feed containing water vapour at temperatures below 100 °C, the two catalysts experienced severe loss of activity. This was accompanied by a loss of microporous volume, but this can likely not alone explain the large deactivation, and in addition the loss was small for the 2.6 wt.% Cu-SAPO-34. Thus, the dominating mechanism for the deactivation does not appear to be the breakage of the crystalline SAPO-34 framework. Further, ammonia storage was unaffected by exposure to water vapour at these low temperatures. We observed a decrease in the TPR signal, indicating that fewer copper sites are available for the redox cycle, and this likely contributes to the deactivation. However, the magnitude of the decrease for the two catalysts was only 26 and 38% (note that 13% of the decrease might originate from alumina present in the deactivated samples) so it seems likely that this is not the only reason for the deactivation, given its severity. We therefore propose that in addition a large number of the copper sites are transformed into an inactive form, and that this transformation is responsible for the loss of SCR activity. The deactivation was not reversed upon attempted regeneration in a dry atmosphere at 600 °C for 35 min.

Acknowledgements

This study was performed at Chemical Reaction Engineering and within the Competence Centre for Catalysis at Chalmers University of Technology. The financial support from the Swedish Research Council is gratefully acknowledged.

References

[1] O. Deutschmann, H. Knözinger, K. Kochloefl, T. Turek, Heterogeneous Catalysis and Solid Catalysts, 1. Fundamentals, Ullmann's Encyclopedia of Industrial Chemistry, Wiley-VCH Verlag GmbH & Co, KGaA, 2000.
[2] J. Li, H. Chang, L. Ma, J. Hao, R.T. Yang, Catal. Today 175 (2011) 147–156.
[3] X. Auvray, W.P. Partridge, J.-S. Choi, J.A. Pihl, A. Yezerets, K. Kamasamudram, N.W. Currier, L. Olsson, Appl. Catal. B 126 (2012) 144–152.
[4] H. Sjövall, R.J. Blint, L. Olsson, Appl. Catal. B 92 (2009) 138–153.
[5] M.H. Kim, I.-S. Nam, Y.G. Kim, Appl. Catal. B 12 (1997) 125–145.
[6] Y. Watanabe, A. Koiwai, H. Takeuchi, S.A. Hyodo, S. Noda, J. Catal. 143 (1993) 430–436.
[7] P. Forzatti, Appl. Catal. A 222 (2001) 221–236.
[8] I. Nova, E. Tronconi (Eds.), Urea-SCR Technology for deNOx After Treatment of Diesel Exhausts, Springer, New York, 2014.
[9] P.G. Blakeman, E.M. Burkholder, H.-Y. Chen, J.E. Collier, J.M. Fedeyko, H. Jobson, R.R. Rajaram, Catal. Today 231 (2014) 56–63.
[10] T. Ishihara, M. Kagawa, F. Hadama, Y. Takita, J. Catal. 169 (1997) 93–102.
[11] J.H. Kwak, D. Tran, S.D. Burton, J. Szanyi, J.H. Lee, C.H.F. Peden, J. Catal. 287 (2012) 203–209.
[12] R. Martínez-Franco, M. Moliner, C. Franch, A. Kustov, A. Corma, Appl. Catal. B 127 (2012) 273–280.
[13] D.W. Fickel, E. D'Addio, J.A. Lauterbach, R.F. Lobo, Appl. Catal. B 102 (2011) 441–448.
[14] F. Gao, J. Kwak, J. Szanyi, C.F. Peden, Top. Catal. 56 (2013) 1441–1459.
[15] M. Briend, R. Vomscheid, M.J. Peltre, P.P. Man, D. Barthomeuf, J. Phys. Chem. 99 (1995) 8270–8276.
[16] J.C. Poshusta, R.D. Noble, J.L. Falconer, J. Membr. Sci. 186 (2001) 25–40.
[17] F. Gao, E.D. Walter, N.M. Washton, J. Szanyi, C.H.F. Peden, ACS Catal. 3 (2013) 2083–2093.

[18] K. Wijayanti, S. Andonova, A. Kumar, J. Li, K. Kamasamudram, N.W. Currier, A. Yezerets, L. Olsson, Submitted (2014).
[19] H. Sjövall, R.J. Blint, L. Olsson, J. Phys. Chem. C 113 (2009) 1393–1405.
[20] Z.-M. Wang, T. Arai, M. Kumagai, Ind. Eng. Chem. Res. 40 (2001) 1864–1871.
[21] R. Vomscheid, M. Briend, M.-J. Peltre, D. Barthomeuf, P.P. Man, J. Chem. Soc. Faraday Trans. 91 (1995) 3281–3284.
[22] F.D.P. Mees, L.R.M. Martens, M.J.G. Janssen, A.A. Verberckmoes, E.F. Vansant, Chem. Commun. (2003) 44–45.
[23] U. Deka, I. Lezcano-Gonzalez, S.J. Warrender, A. Lorena Picone, P.A. Wright, B.M. Weckhuysen, A.M. Beale, Microporous Mesoporous Mater. 166 (2013) 144–152.
[24] D. Wang, L. Zhang, J. Li, K. Kamasamudram, W.S. Epling, Catal. Today 231 (2014) 64–74.
[25] L. Wang, J.R. Gaudet, W. Li, D. Weng, J. Catal. 306 (2013) 68–77.
[26] N. Wilken, R. Nedyalkova, K. Kamasamudram, J. Li, N. Currier, R. Vedaiyan, A. Yezerets, L. Olsson, Top. Catal. 56 (2013) 317–322.
[27] K. Leistner, F. Brüsewitz, K. Wijayanti, A. Kumar, J. Li, K. Kamasamudram, N.W. Currier, A. Yezerets, L. Olsson, unpublished work.
[28] P.N.R. Vennestrøm, A. Katerinopoulou, R.R. Tiruvalam, A. Kustov, P.G. Moses, P. Concepcion, A. Corma, ACS Catal. 3 (2013) 2158–2161.
[29] H. Jääskeläinen, Diesel Exhaust Gas, Diesel Exhaust Gas, DieselNet.
[30] J.A.Z. Pieterse, R.W. van den Brink, S. Booneveld, F.A. de Bruijn, Appl. Catal. B 39 (2002) 167–179.
[31] F.G. Requejo, J.M. Ramallo-López, E.J. Lede, E.E. Miró, L.B. Pierella, O.A. Anunziata, Catal. Today 54 (1999) 553–558.